Aalto University
School of Chemical
Technology

Structural and Electronic Analysis of $Li_xMn_2O_4$ by XAS:

A Case Study for XANES and EXAFS Analysis

M.Sc. Daniel Settipani
Aalto University (Finland)

XAS Workshop and Training 2018
University of Helsinki, Finland
11th June 2018

OUTLINE

PART 1

INTRODUCTION

1.1 Academic Background
1.1 Lithium-ion batteries
1.2 β – MnO_2, $LiMn_2O_4$, Rutile to spinel transformation
1.3 Research objective
1.4 XAS: XANES, EXAFS

PART 2

EXPERIMENTAL PROCEDURE

2.1 Sample preparation
2.2 Thin-film characterization

PART 3

RESULTS

3.1 XANES region
3.2 EXAFS region

PART 4

CONCLUSIONS, REMARKS, RECOMMENDED LITERATURE

INTRODUCTION

Academic Background

- **Materials Engineer Cum Laude** (2015), Simón Bolívar University, Caracas, Venezuela.
- Spec.: Structural-industrial ceramics, characterization techniques, metals
- Exchange studies: Krakow, Poland at AGH
- Thesis: Limoges, France at IMERYS Ceramics

- **M.Sc. in Materials Science** (2017), Université de Rennes 1 (Rennes, France) & Università di Torino (Turin, Italy)
- Spec.: Synchrotron and neutron radiation sources, spectroscopic methods, crystallography
- Thesis: University of Helsinki (Aim: *Get further fundamental information about the ALD processing of lithium-containing materials, and specifically, of the rutile to spinel transformation of ALD-MnO_2 to produce $Li_xMn_2O_4$ spinel cathode materials)*

- **PhD student** (autumn-2018), ESR Fellow at Aalto University, Dept. Of Chemistry and Materials Science.
- Topic: *ALD-synthesis and characterization of metal oxide electrocatalysts for the oxygen evolution reaction (OER) (http://www.elcorel.org)*

Lithium-ion batteries (LIBs)

- Highest energy density→ dominating the rechargeable batt. market

G. Jian, S. Si-Qi, L. Hong. 2016. Brief overview of electrochemical potential in lithium ion batteries. Chinese Physics B. 2016 25 (1): 018210. DOI: 10.1088/1674-1056/25/1/018210

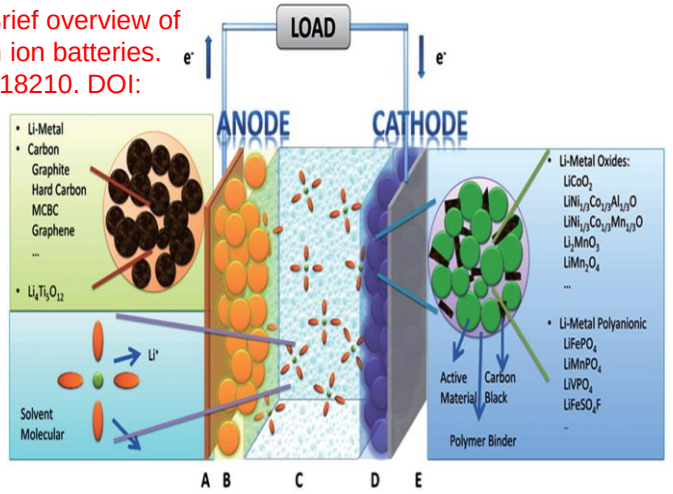

- LIBs = Anode + Electrolyte + Cathode

- Operation principle → Intercalating/de-intercalating Li-ions

- **Anode** → Li-Ion intercalation electrode (generally graphite)
  Electrolyte → Li-Ion conducting electrolyte
  (Ex: $LiPF_6$ in ethylene carbonate-diethylcarbonate)
  Cathode→ Li-Ion intercalation electrode
  (Transition Metal Compounds: $LiCoO_2$, $LiNiO_2$, **$LiMn_2O_4$**)

- Cathode material → Limiting factor to the electrochemical performance

- ALD process → Enabling technology for 3D all solid state thin-film LIBs

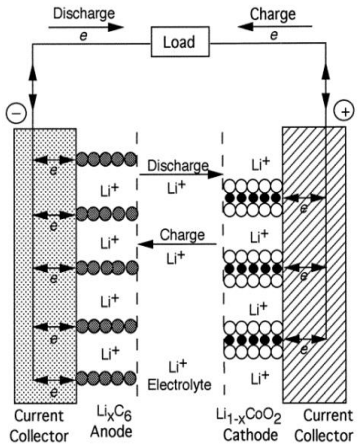

T. Eriksson. 2001. LiMn 2 O 4 as a Li-Ion Battery Cathode. From Bulk to Electrolyte Interface. (Doctoral thesis). Acta Universitatis Upsaliensis. Comprehensive Summaries of Uppsala Dissertations from the Faculty of Science and Technology 651. 53 pp. Uppsala University. ISBN 91-554-5100-4

Lithium-ion batteries (LIBs)

$LiMn_2O_4$:

- Low cost, low toxicity, environmental favorable (in comparison to Co-, Ni-based chemistries)
- High specific theoretical capacity → 148 $mAhg^{-1}$ (function well in the 4V region)
- Minimal structural changes during charge/discharge cycling → **Spinel Framework**

$LiMn_2O_4$:

- Capacity loss on charge-discharge cycling (cyclabilit
- Low energy density (only 0.5 Li ions can be intercala oxide contains Mn $^{3+}$ and Mn $^{4+)}$
- $Li_2Mn_2O_4$ leads to a marked loss of capacity due to tl the lattice parameters on formation of the tetragonal

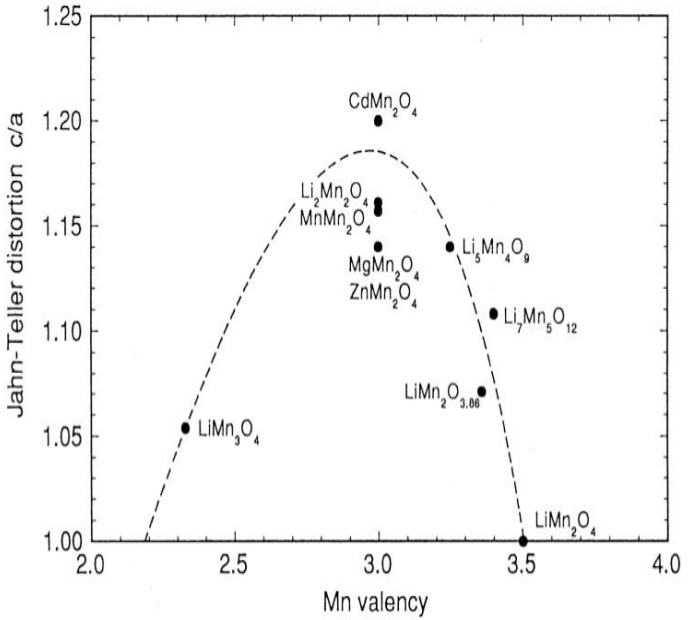

A. Yamada. 1996. Lattice Instability in Li(Li x Mn 2-x 122, Issue 1, 160-165. DOI: 10.1006/jssc.1996.0097

Rutile to spinel transformation

- **W.I.F. David *et al.* (1984):** W.I.F. David, M. M. Thackeray, P. G. Bruce, J. B. Goodenough. 1984. Lithium insertion into β-MnO 2 and the rutile-spinel transformation. Mat. Res. Bull. 1984, Volume 19, pp. 99-106. DOI: 10.1016/0025-5408(84)90015-1
- Bulk rutile MnO_2 can be coverted to $Li_xMn_2O_4$ by treating with hexane solution of n-butyl lithium for 170 hours at 50-60 ºC
- **Miikkulainen *et al.* (2014):** V. Miikkulainen, A. Ruud, E. Østreng, O. Nilsen, M. Laitinen, T. Sajavaara, H. Fjellvåg. 2014. Atomic layer deposition of spinel lithium manganese oxide by film-body-controlled lithium incorporation for thin-film lithium-ion batteries. J. Phys. Chem. C. 2014 118 (2) 1258–1268. DOI: 10.1021/jp409399y
- ALD-MnO_2 thin-film was successfully converted into a $Li_xMn_2O_4$ spinel by applying cycles of Li(thd) + O_3 or LiO^tBu + H_2O at 225 ºC on top of the parent film.

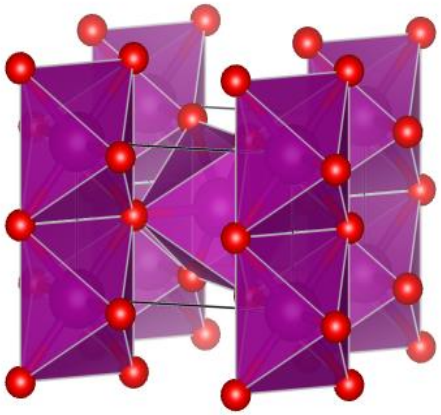

Pyrolusite
[MnO6] framework (sharing egdes/corners)

Lithiation

Reducing agent

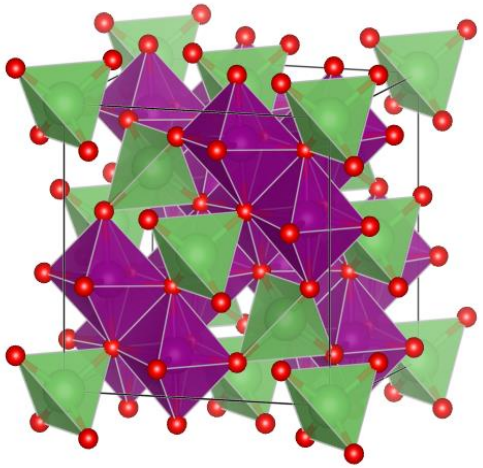

[Mn_2O_4] framework
([MnO6] edge sharing)

Research objective

- LIBs Electrochemical properties (charge capacity and charge retention) → Influenced by: Crystallographic and oxidation state of the metal element in the cathode material.

✓ Investigation of atomic and electronic structure → Significant interest

Main objective:

Investigate the structural and electronic changes near the Mn atom during the conversion of an ALD-MnO_2 thin-film into $Li_xMn_2O_4$ spinel, upon lithium insertion due to gas-solid reactions.

- X-Ray Absorption Spectroscopy (XAS):

1. X-Ray Absorption Near-Edge Structure (XANES) → Mn average oxidation state (AOS)
2. Extended X-Ray Absorption Fine Structure (EXAFS) → Geometrical structure around the Mn atom (e.g. Mn-ligand average distances)

X-ray absorption spectroscopy (XAS)

E. Borfecchia, D. Gianolio, G. Agostini, S. Bordiga, C. Lamberti. 2013. Characterization of MOFs. 2. Long and Local Range Order Structural Determination of MOFs by Combining EXAFS and Diffraction Techniques. In: F. X. Llabrés i Xamena, J. Gascon (Editors). Metal Organic Frameworks as Heterogeneous Catalysts. The Royal Society of Chemistry. 2013. Chapter 5 p. 143-208. DOI: 10.1039/9781849737586

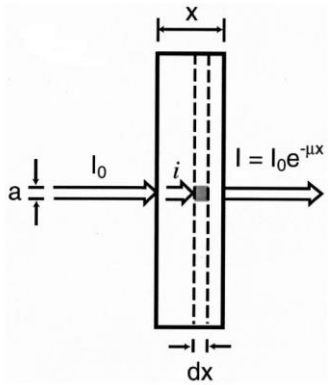

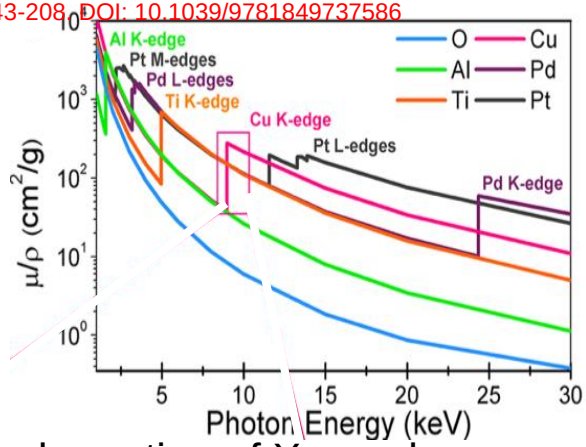

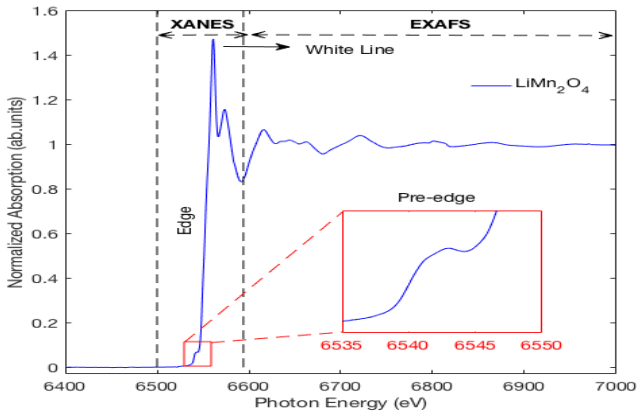

- XAS → Photoelectric absorption of X-rays by core electrons
- XAS → Quantitative measurement of μ (E) → Absorption coefficient in a sample as a function of the incoming photon energy.
- Core electrons → element-specific energies → Absorption edges
- XANES region→ oxidation, coordination state and symmetry of the absorbing atom.
- EXAFS region→ Local structure surrounding the absorbing atom (types and numbers of atoms in coordination with the absorber, their interatomic distances, and their degree of static and thermal disorder)

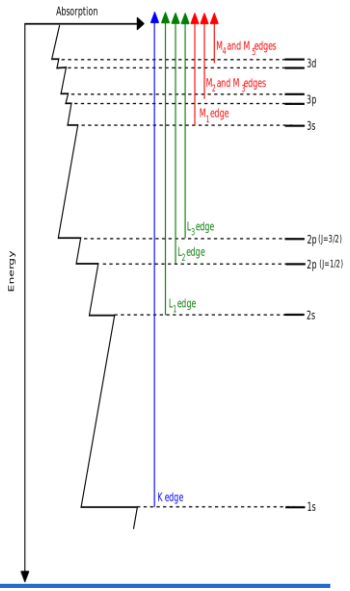

XANES region

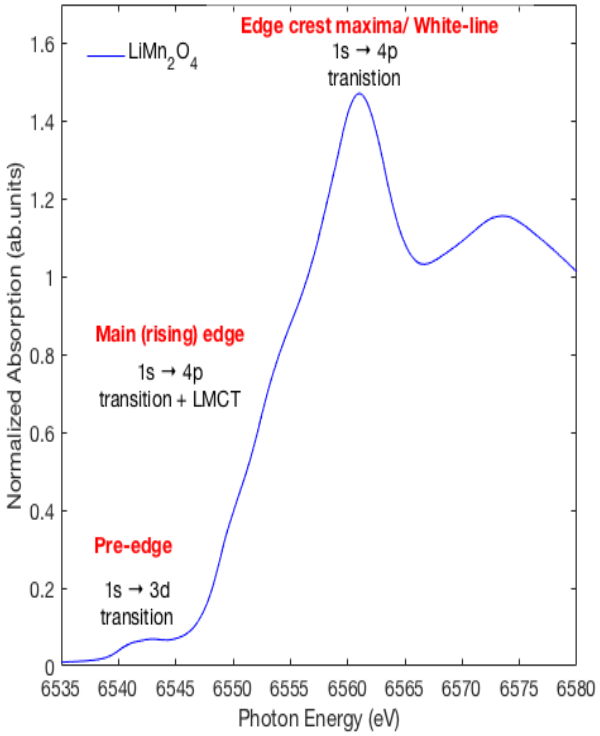

- Signal → electronic transitions to unoccupied bound states, to nearly bound states, and to the continuum.
- Ranges from approx. -50 to about 200 eV relative to the absorption edge energy. (e.g. Absorption Mn K-edge energy of 6539 eV)
- Two main regions: Pre-edge + Edge region
- Shifts *(chemical shifts)* in the absorption features → Average effective charge of the absorbing atom (Zeff) → Average Oxidation State (AOS)
- Shifts also influenced by ligand environment around the absorber (e.g. # surrounding ligands, metal-ligand bond distances, site symmetry, orbital mixing)
- Intensity of absorption features → Local site symmetry and orbital occupancy
- Shape of the spectra → Influenced by ligand environment around the absorber

XANES region

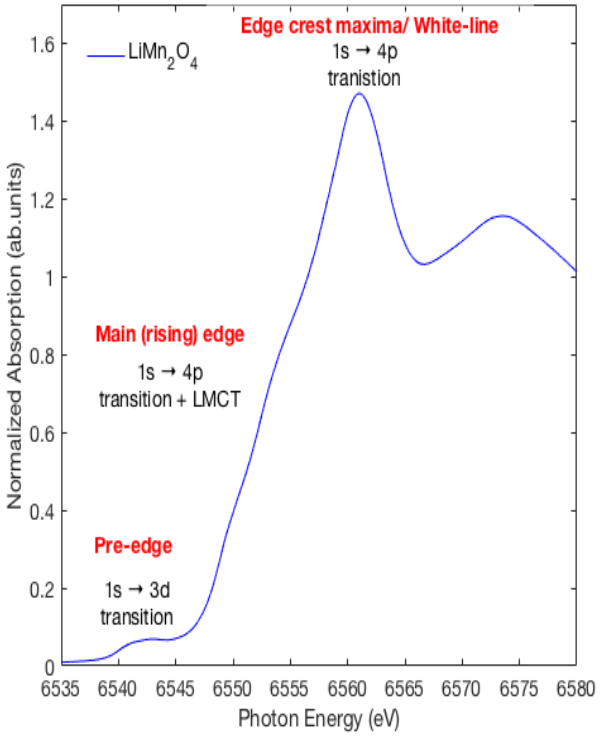

- For a $LiMn_2O_4$ spinel samples:
- Pre-edge region → 1s →3d transitions,
- Rising edge region → 1s →4p + LMCT transitions
- Edge crest maxima → Purely dipole-allowed 1s → 4p transitions.
- The intensity of edge crest peak is proportional to the relative concentration of edge-shared $[MnO_6]$ octahedra with respect to corner-shared ones

EXAFS region

J. Als-Nielsen, D. McMorrow. 2011. Elements of Modern X-ray Physics, Second Edition. John Wiley & Sons, Inc. DOI: 10.1002/9781119998365.biblio

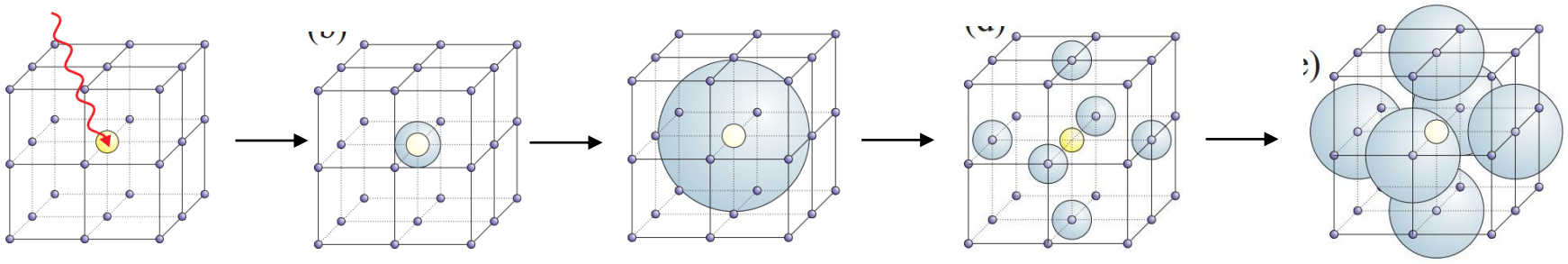

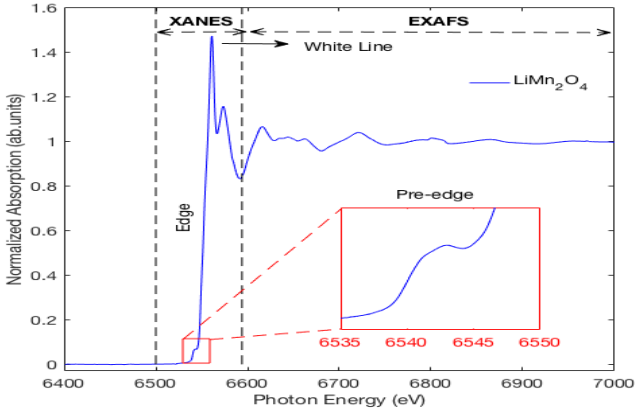

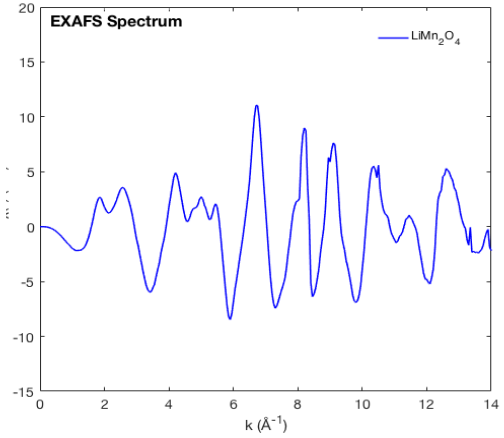

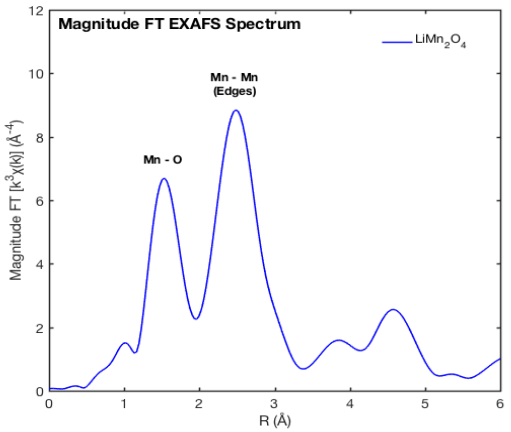

- Signal → Quantum-mechanical interference of the ejected and propagating photoelectron wave with the electrons of neighboring atoms → **<u>Oscillatory modulation of absorption coefficient</u>** → Information about the local atomic structure around the absorbing atom.
- Fourier transform + Data fitting → Quantitative information → Types and numbers of atoms in coordination with the absorber, interatomic distances, degree of static and thermal disorder

EXAFS region

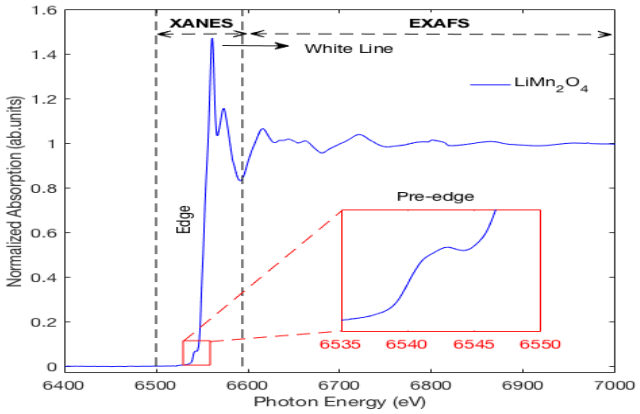

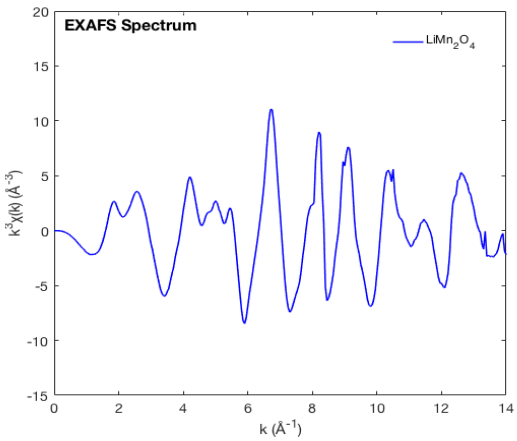

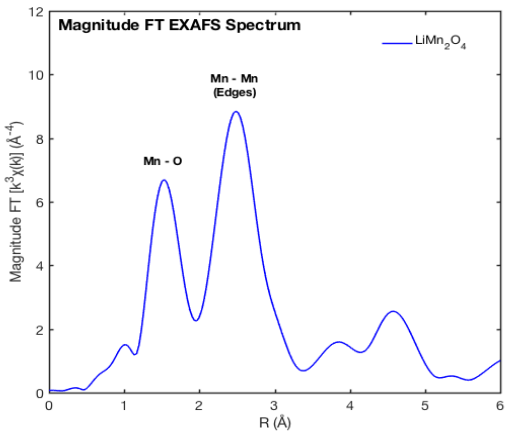

- Oscillations will be smoothed at higher energies → Only local structural information of the nearest neighbors (up to 5 – 8 Å)
- The signal is extracted from the total spectrum following :

$$\chi(E) = \frac{\mu(E) - \mu_0(E)}{\Delta\mu_0(E)}$$

- Since oscillations occur above the absorption edge, "χ(E)" can be substituted with the photoelectron wavector "k", and therefore, the EXAFS signal can be expressed as χ(k)

M. Siebecker. 2016. Online workshop: A Practical Workshop on EXAFS Shell Fitting for Environmental Samples Part 1 and Part 2. Online workshop hosted by the Delaware Environmental Institute of the University of Delaware. Available at: https://www.youtube.com/watch?v=Il_wRqhqFM4&t=3645s

EXAFS region: Fitting Procedure

- EXAFS signal → Sum of sine waves (each with a phase and amplitude) coming from all scattering paths of the photoelectron
- The red parameters affect the amplitude of the EXAFS oscillations
- The blue parameters affect the phase of the EXAFS oscillations

$$\chi_i(k) \equiv \frac{\left(N_i S_0^2\right) F_{\mathrm{eff}_i}(k)}{kR_i^2} \sin\left[2kR_i + \varphi_i(k)\right] e^{-2\sigma_i^2 k^2} e^{\frac{-2R_i}{\lambda(k)}}$$

$$R_i = R_{0i} + \Delta R_i$$

$$k^2 = \frac{2m_e\left(E - E_0 + \Delta E_0\right)}{\hbar}$$

N – coordination number (CN), (4, tetrahedral, 6 octahedral)
S_0^2 – Amplitude reduction factor ("es-oh-tu")
σ^2 – the disorder term ("sigma squared")
ΔE – the change in energy from theoretical data ("delta E")
ΔR – the change in interatomic distance ("delta R")

EXAFS region: Fitting Procedure

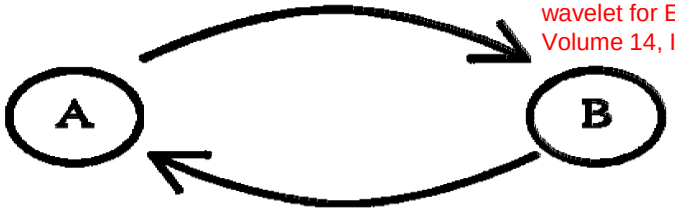

H. Funke, M. Chukalina, A. C. Scheinost. 2007. A new FEFF-based wavelet for EXAFS data analysis. J. Synchrotron Radiation. 2007, Volume 14, Issue 5, p. 426-432. DOI:10.1107/S0909049507031901

A single scattering path (back and forth)

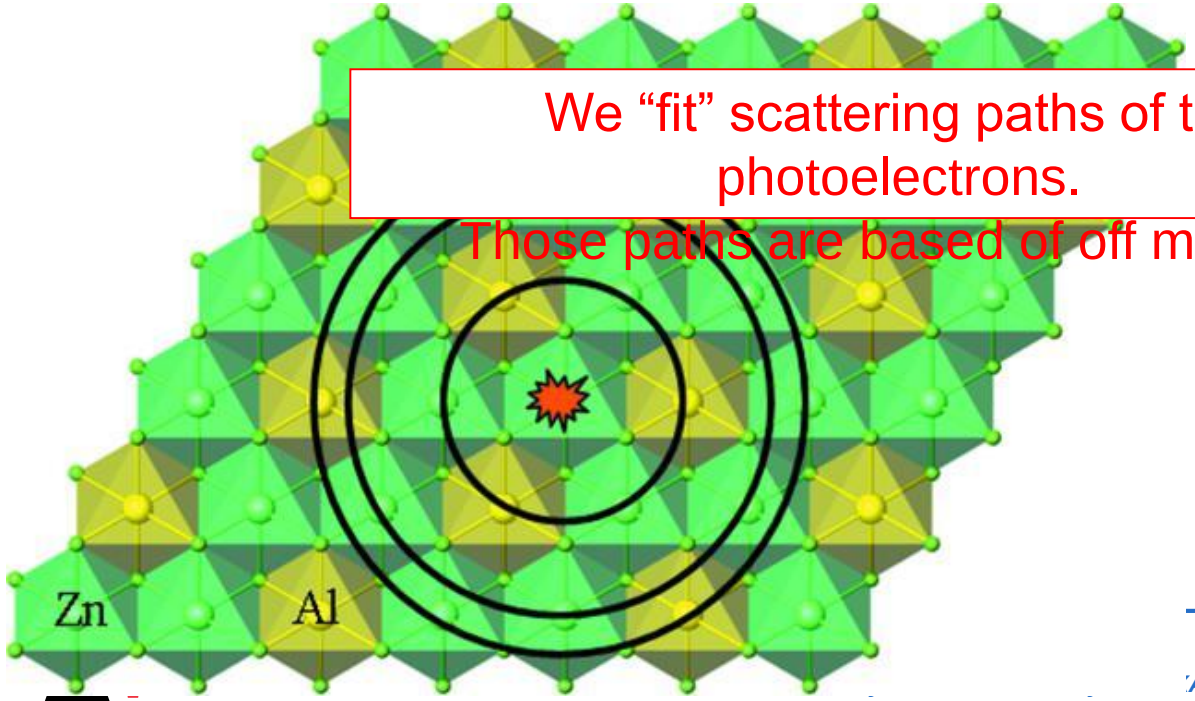

We “fit” scattering paths of the photoelectrons.

Those paths are based of off models.

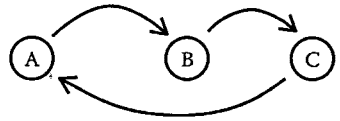

Figure 14.5 A focused path.

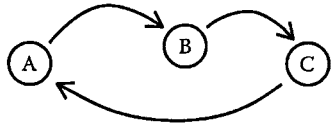

Figure 14.6 A partially focused path.

Figure 14.7 A double path.

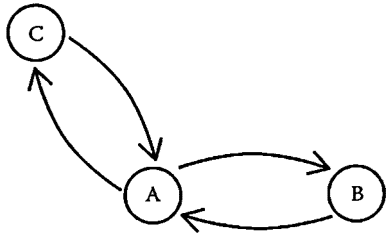

Figure 14.8 A conjoined path.

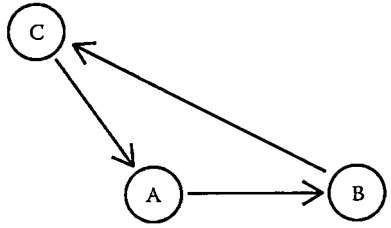

Figure 14.9 A triangle path.

EXAFS region: Fitting Procedure

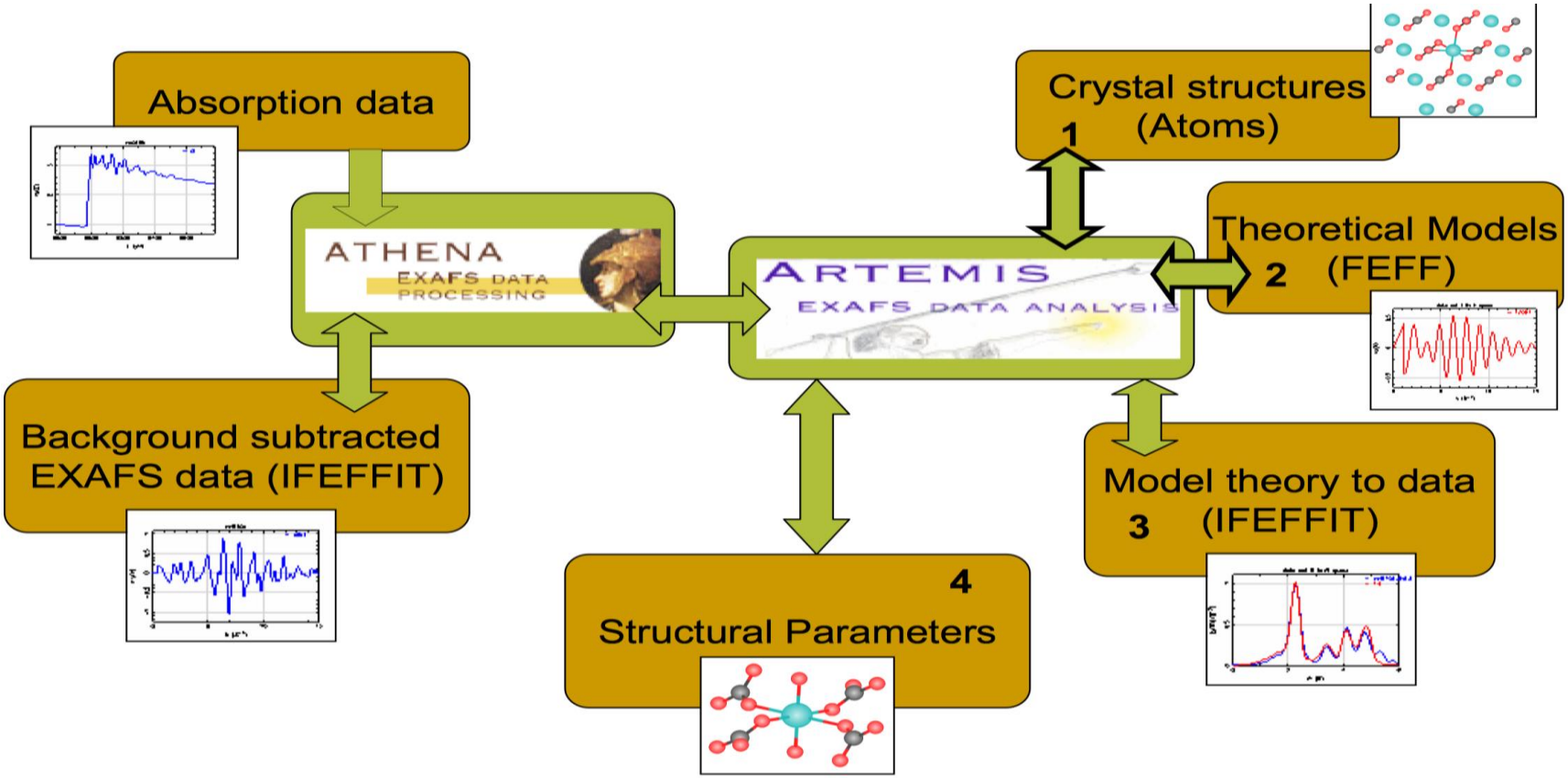

http://xafs.org/Tutorials?action=AttachFile&do=get&target=Basics_of_XAFS_analysis.pdf

- Crystal structure (models): β-MnO_2 and $LiMn_2O_4$;
- Δk = 2.912 – 11.671 $Å^{-1}$; ΔR = 0.92 – 2.5 Å and 0.92 – 3.4 Å ($LiMn_2O_4$)

EXAFS region

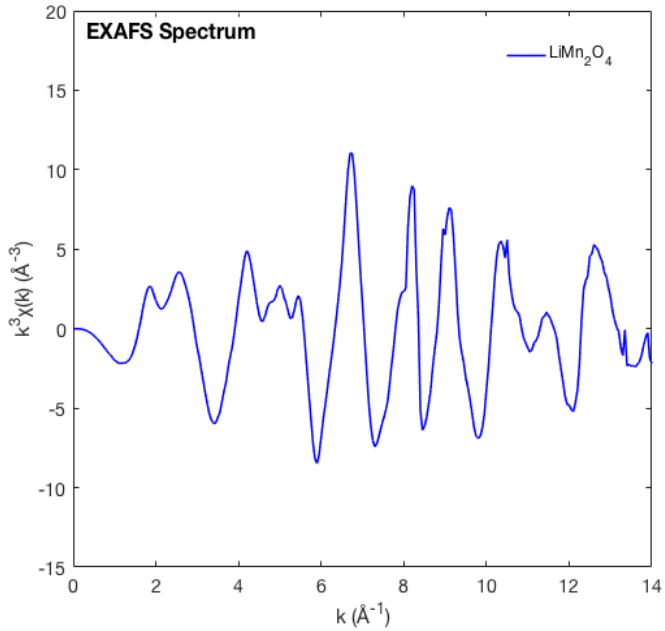

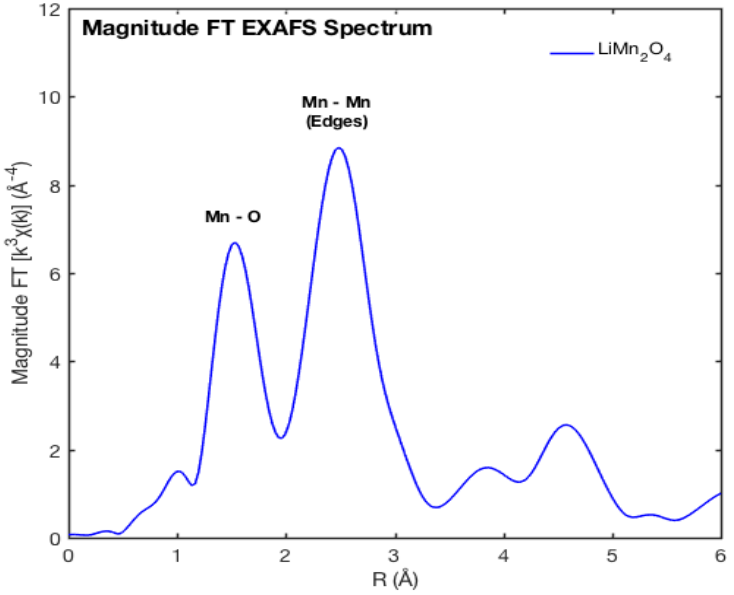

- 1st peak in “R-space” plot → Nearest 6 O atoms (first coordination shell) → Mn-O distances in the $[MnO]_6$ octahedron
- 2nd peak in “R-space”plot → Nearest 6 Mn atoms (second coordination shell) → Mn-Mn distances → Mn in octahedra sharing edges with the $[MnO]_6$ octahedron
- 3-Dimensional framework → $[Mn_2O_4]$ → Multiple scattering specially due to *focusing effect* due to distant Mn atoms.

EXPERIMENTAL PROCEDURE

Sample Preparation

- 9 lithiated samples ($Li_xMn_2O_4$)
- Procedure → ALD-MnO_2 + Lithiation cycles
- **ALD-MnO_2:**

Temperature of deposition: 225 ºC

Deposition cycles: 5000

Precursors: $Mn(thd)_3$ (0.5-s pulse/3-s purge) + O_3 (5-s pulse/5-s purge). The temperature of the $Mn(thd)_3$ was 160 ºC and the O_3 partial pressure was 14 hPa. The ozone was produced by a *Wedeco* generator.

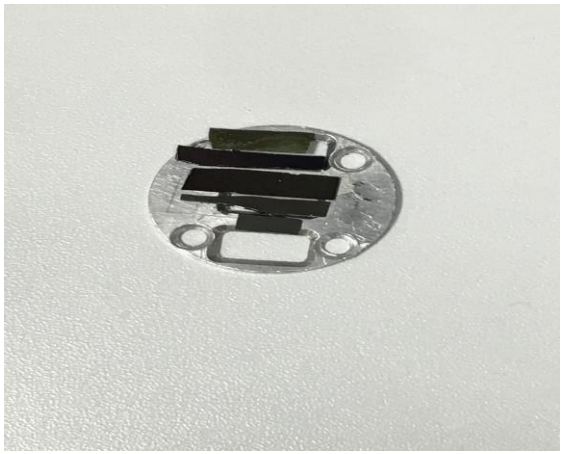

- **$Li_xMn_2O_4$:**

Temperature of deposition: 225 ºC

Deposition cycles: 10, 50, 100, 200 and 300.

Precursors: LiO^tBu (0.5-s pulse/5-s purge) + H_2O (0.1-s pulse/10-s purge). The temperature of the LiO^tBu was 160 ºC.

Annealing procedure: Annealing at 400 ºC and/or 600 ºC during 10 min in N_2.

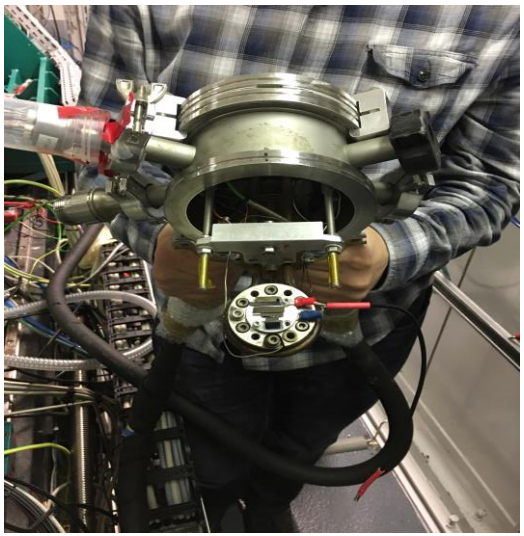

Thin-Film Characterization

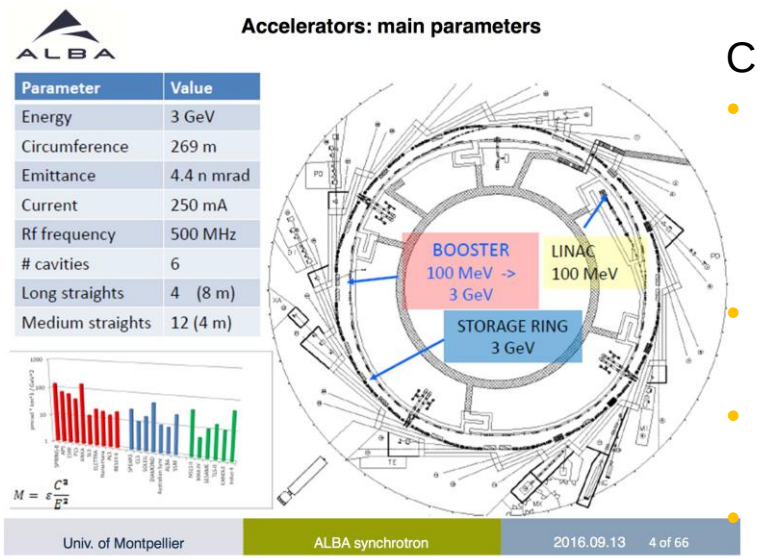

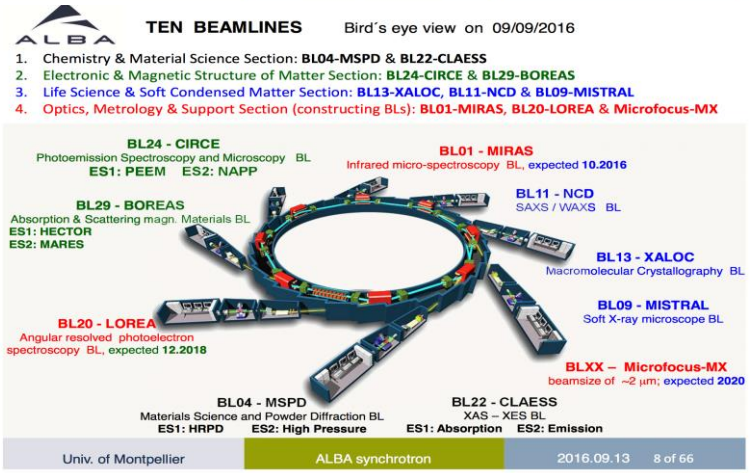

CLAESS beamline:

- Mn K-edge (6539eV) in transmission mode (references), TFY and TEY (fluorescence and by collecting the sample drain current)
- Spectra will be collected up to k ~ 18 Å $^{-1}$ (7750eV)
- Data reduction and analysis → ATHENA + ARTEMIS
- RT= 27.7ºC (cooling with LN_2)

Staff: Laura Simonelli (Italian)
Carlo Marini (Italian)
Wojciech Olszewski (Polish)
Nitya Ramanan (Indian)

RESULTS

Results – XANES Region

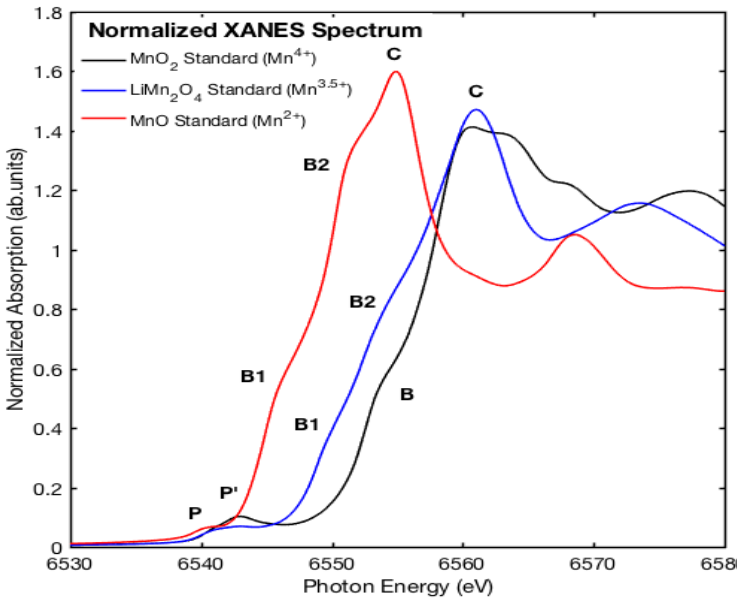

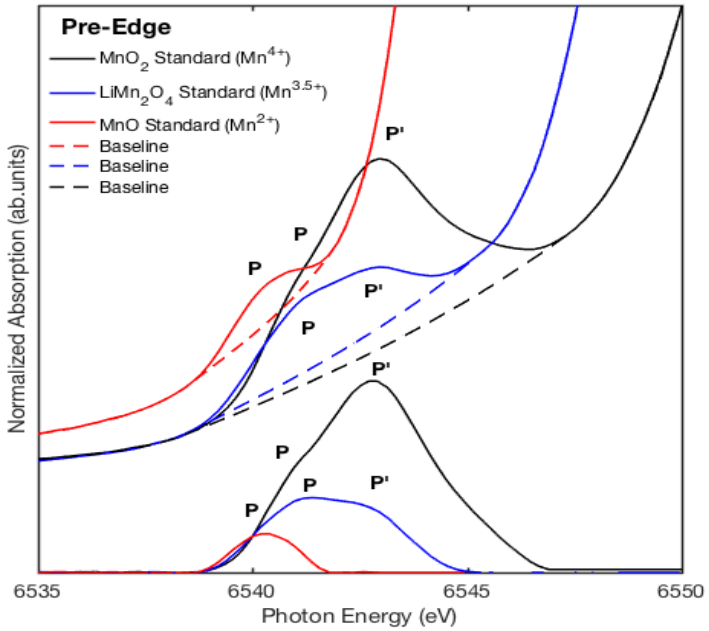

- Low pre-edge intensities → Mn ions in octahedral sites
- Multiplet structure due to splitting of 3d levels (e.g. t_{2g} and e_g)
- Higher and more broaden pre-edge areas → Increase of Mn AOS and site distortion (i.e.. MnO → $LiMn_2O_4$ → MnO_2)
- Edge absorption features shift to higher energies with increase of Mn AOS (qualitative estimation)

Results – XANES Region

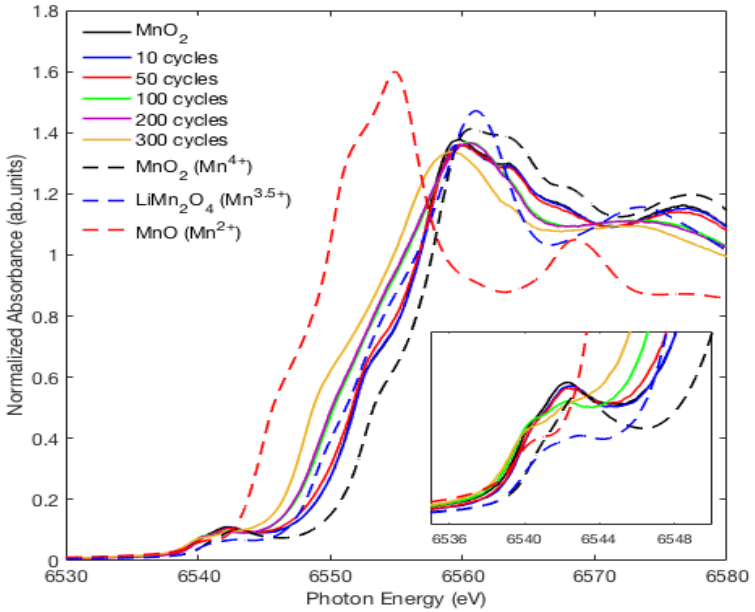

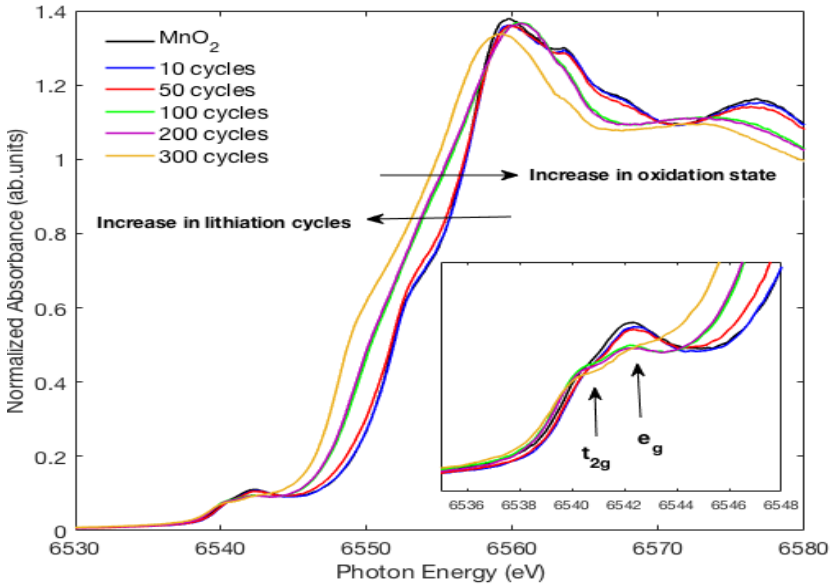

- Shift in the main edge → Reduction of Mn atom as MnO_2 is converted to $Li_xMn_2O_4$ (even at low lithiation cycles)
- ALD-MnO_2, 10-50 cycles → Similar in shape → Similar chemical environment
- MnO_2 to $Li_xMn_2O_4$ is favored from 100 cycles upwards.
- 100 cycles and 200 cycles → Similar in shape to reference $LiMn_2O_4$
- The Mn atom on the 300 cycle seems to have different chemical environment

Results – XANES Region

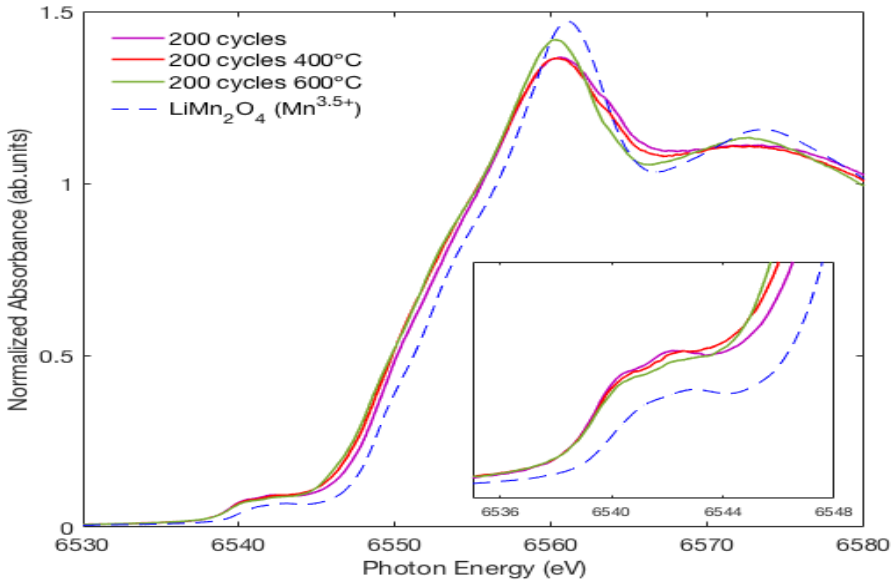

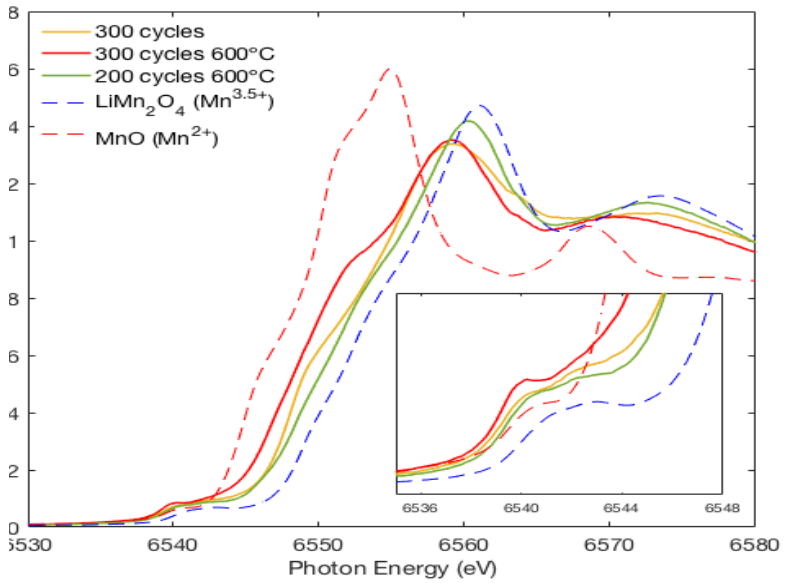

- No relative change in Mn local environment upon annealing of the 200c (Only a slight reduction and slight decrease of pre-edge peak intensity with increasing T)
- 300 cycles sample → The overall shape changes upon annealing (its pre-edge feature appears similar but more intense to the one in the MnO reference)

Results – XANES Region

- **In summary:**
- Overall **decrease in edge-energy position** upon lithium insertion indicates a **reduction of the average oxidation state** of the Mn.

- **Decrease in intensity of the pre-edge peaks** upon lithium insertion → Also indicates the presence of **lower average oxidation states.**

- For the 10 and 50 cycles samples, the site symmetry around of the Mn atom is similar to the one found in the reference sample of MnO_2 .

- Upon increasing lithiation (i.e., in the 100, 200 and 300 cycles samples), the shape of the pre-edge features changes and is similar to the one found in $LiMn_2O_4$ spinel reference sample.

- (Pre-edge features) For the 200 cycles samples, it appears that the symmetry of the site doesn't change too much with annealing temperatures, however, for the 300 cycles sample, there is a significant change in local geometry when the sample is annealed.

Results – XANES Region (Mn AOS)

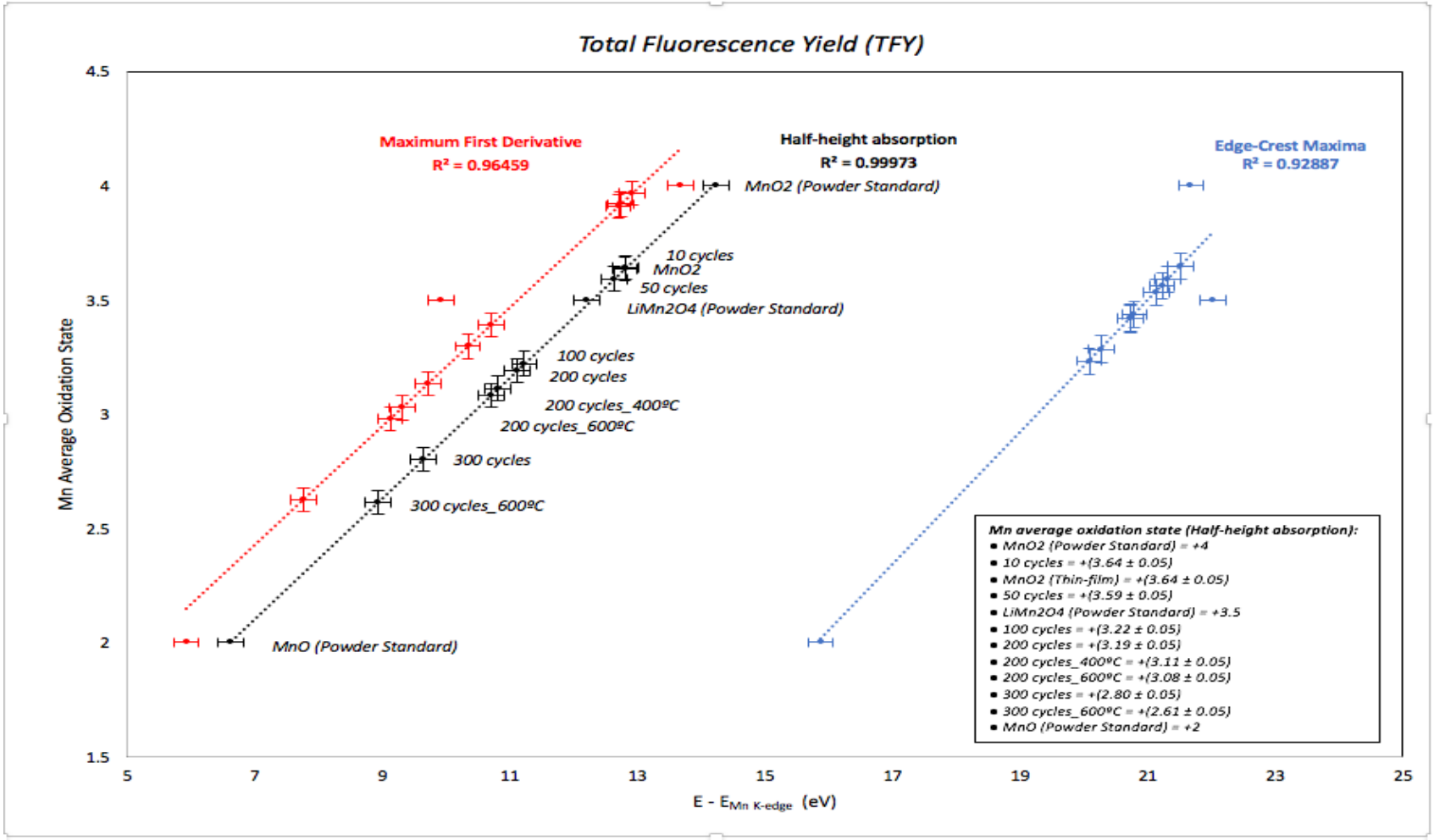

Results – XANES Region (Mn AOS)

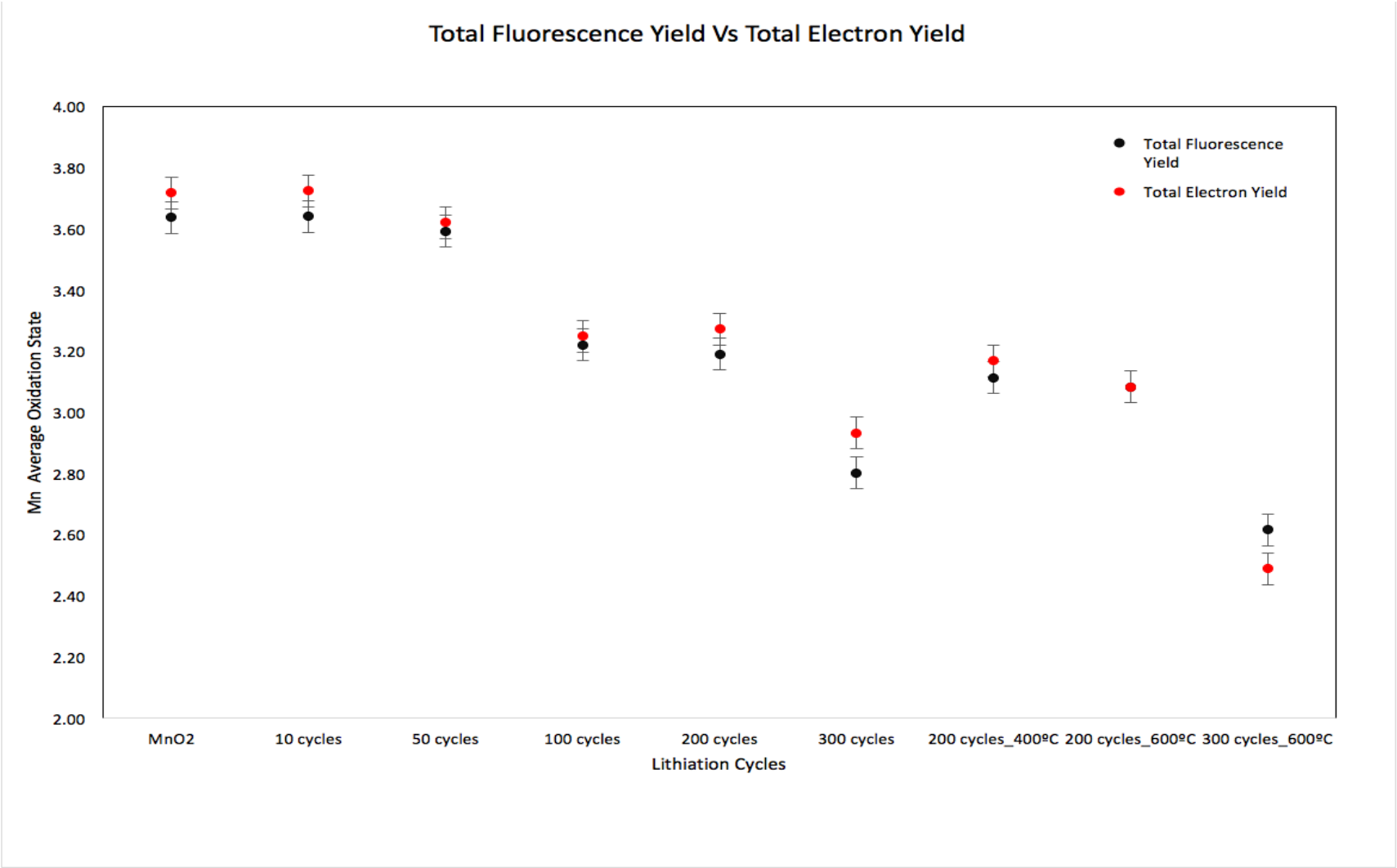

Results – XANES Region

- **In summary:**
- Energy shifts of various absorption features are plotted against the formal average oxidation state of Mn to estimate the change in Mn AOS

- The absorption features that best follows the lineal correlation with oxidation state of the absorbing atom are the ones located in the edge of the spectrum. → The “half-height” absorption feature is the one with the best “R-factor”, and is the one used to assess the change in average oxidation state.

- Upon lithium insertion, the average oxidation state of the Mn reduces from ≈ 3.6+ (in thin-film MnO_2) to ≈ 2.8+ (in the 300 cycles thin-film sample).

- There is no apparent difference in the average oxidation state between the bulk and surface of the sample.

- However, the estimation of the AOS by the XANES analysis is prone to larger errors (i.e. chemical shifts are not only influenced by changes in AOS)

Results – EXAFS Region

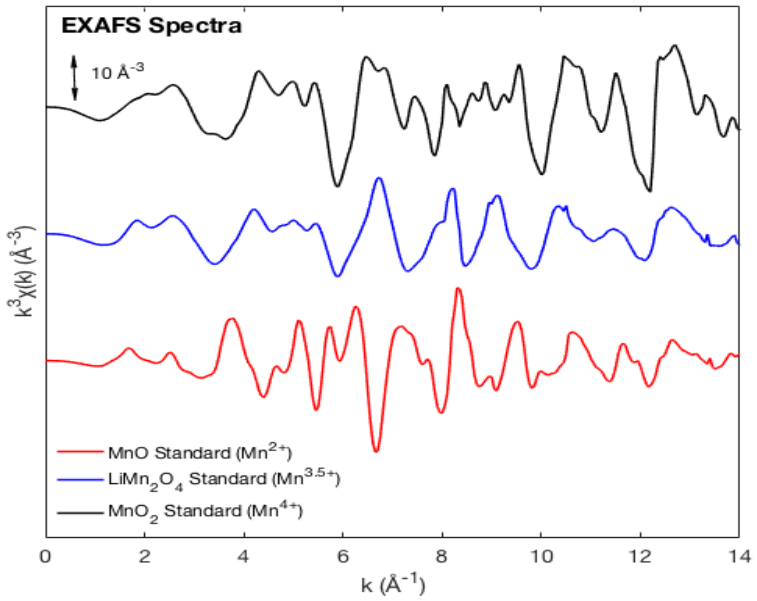

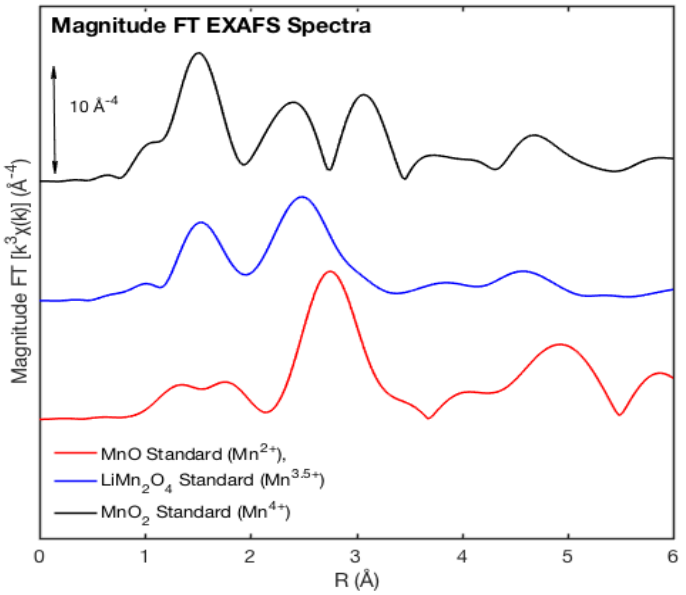

- MnO_2 reference → 1st (Mn-O) interaction, a 2nd peak related to the (Mn-Mn) interaction between edge-shared [MnO6] octahedra, and a 3rd related to a (Mn-Mn) interaction between corner-sharing [MnO6] octahedra.

- $LiMn_2O_4$ reference → 1st peak related to a (Mn-O) interaction, and a 2nd peak related to the (Mn-Mn) interaction between edge-shared [MnO6] octahedra.

Results – EXAFS Region

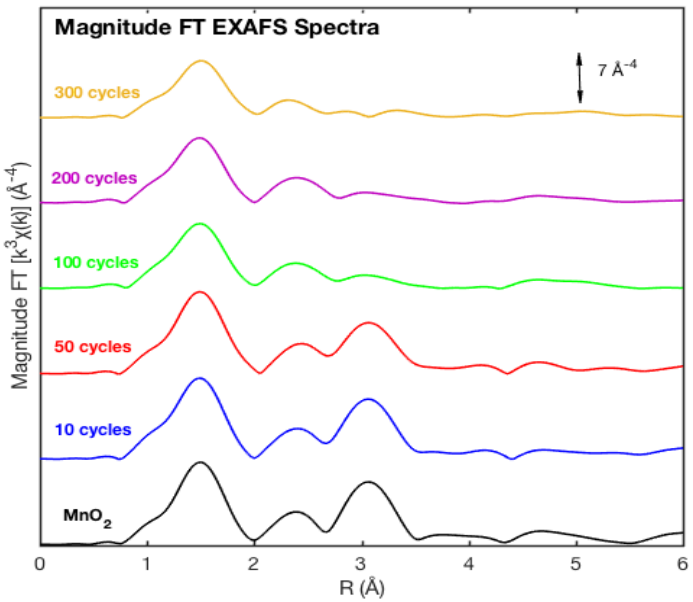

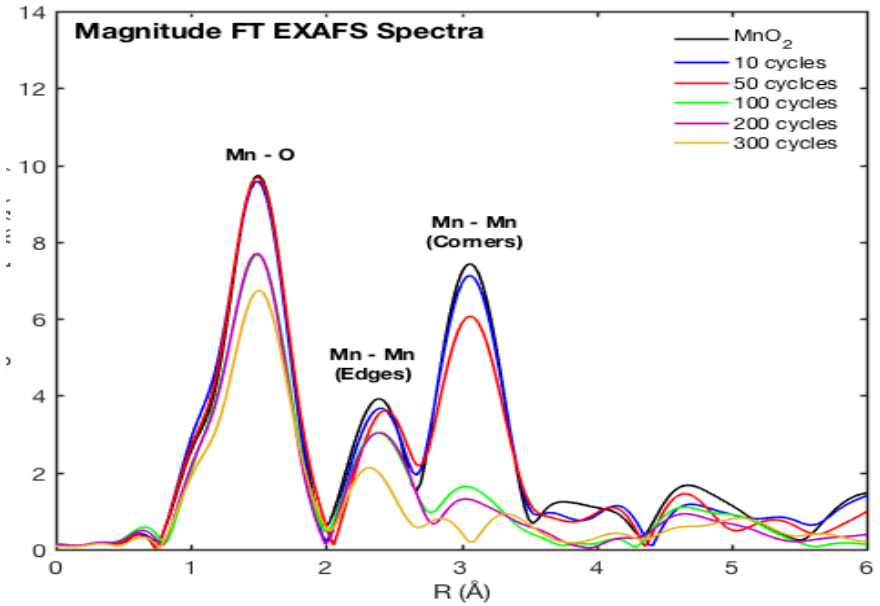

- The rutile to spinel transformation of MnO_2 into a spinel like phase of $Li_xMn_2O_4$ is apparent from 100 cycles upwards.
- The reduction in amplitude of the 1st and 2nd peak is evidence of increase in local disorder around the Mn atom (i.e. absorber) upon lithiation

Results – EXAFS Region

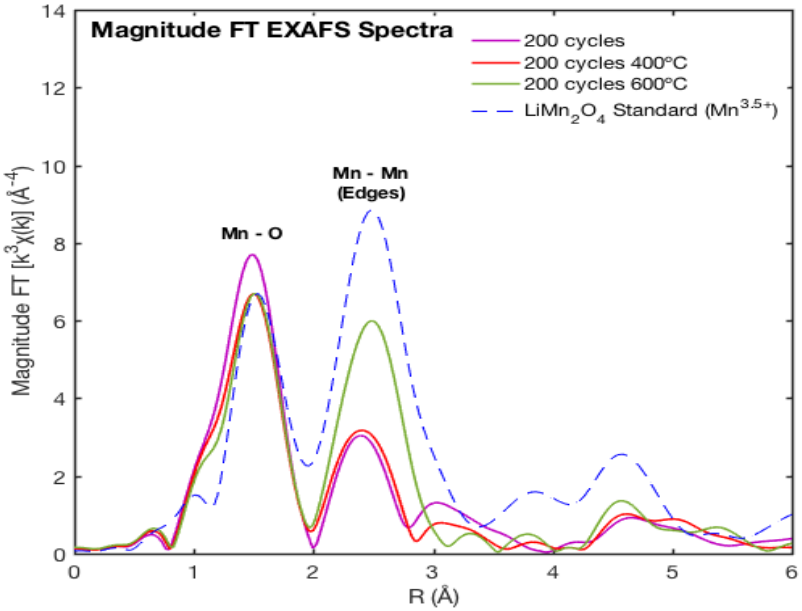

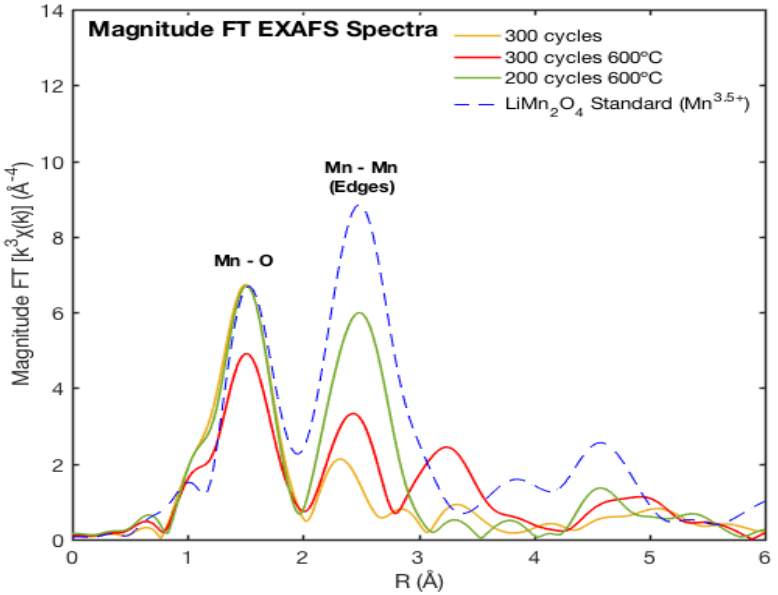

- Upon increasing annealing temperature, the intensity of the 2nd coordination peak of the 200 cycles sample is increased → Local ordering and crystal structure is closer to the reference $LiMn_2O_4$
- Presence of 3rd coordination peak on the 300 cycles sample upon annealing → Not expected in a $LiMn_2O_4$ spinel material with Oh symmetry

Results – EXAFS Region

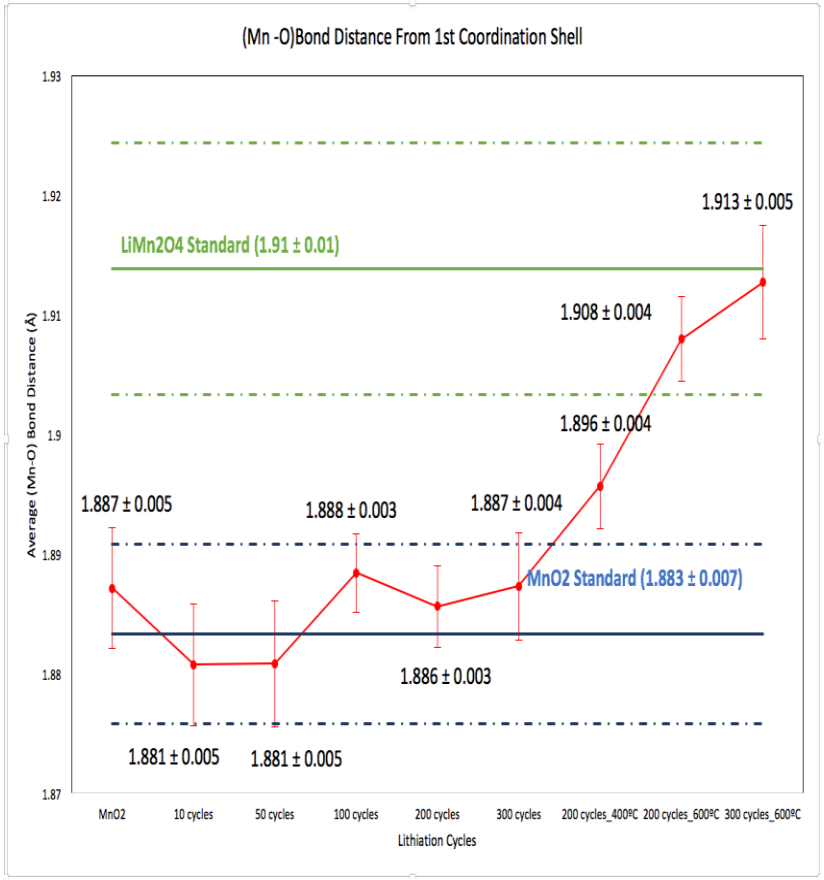

- EXAS data fitted with two theoretical models:

1) MnO_2 (pyrolusite)
2) Spinel $LiMn_2O_4$

- Refined values of Mn-O bond length were plotted to observe the changes (local distortion) upon lithium insertion and for correlation with the changes in Mn AOS

- Remarks:

Mn 3+ ions → 0.645 Å ;
Mn 4+ ions → 0.530 Å

Results – EXAFS Region

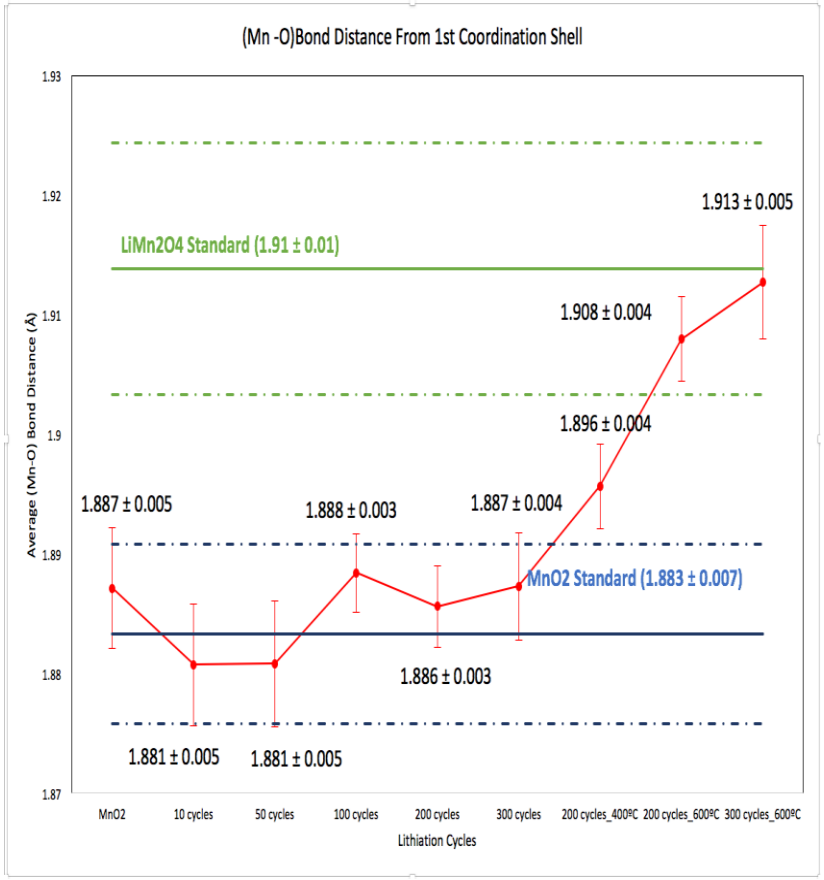

- There is an increase of average Mn-O bond length upon increasing lithiation → Supports observation by XANES → Reduction of Mn AOS upon increasing lithiation cycles
- This reduction is not the same as the one evidence in the XANES analysis. According to the EXAFS analysis, there is reduction from about Mn 4+ to about Mn 3.5+ when going from the MnO_2 thin-film sample to the 300 cycles 600ºC
- From the XANES analysis the reduction goes from about Mn 3.6+ to Mn 2.6+ .

CONCLUSIONS & FINAL REMARKS

Conclusions

- From **both XANES and EXAFS analysis**, it was demonstrated that the **AOS of Mn decreases as a function of lithiation cycles**, with no apparent large differences between the bulk and surface of the samples. It appears that the conversion from rutile to spinel is activated from 100 cycles onwards.

- This local distance **"Mn-O "distance appears to be slightly longer and increasing** for **more lithiated samples** due to the Mn reduction.

- For more **lithiated samples**, there is **reduction** of the corner-sharing octahedra **[MnO6] upon lithiation**.

- The changes in the Mn – O bond distances are in good correlation with the chemical shifts in the XANES spectra. However**, the changes in bond distances correlate to a "lower" reduction of the oxidation state upon increasing lithiation** cycles than in the case of the XANES analysis.

- The 200 cycles 600ºC sample is the one closer, in terms of crystal structure, to the expected $LiMn_2O_4$ spinel phase.

Remarks

- To get a more accurate and quantitative estimation of the Mn redox state the pre-edge absorption features should be extensively studied. A analysis methodology involving the modeling of the pre-edge features together with ab initio multiple-scattering calculations and density functional theory (DFT) based methods is recommended.

.

Recommended Literature

- S. Calvin. 2013. XAFS for Everyone. CRC Press. ISBN 978-1-4398-7864-4
- F. de Groot, A. Kotani. 2008. Core Level Spectroscopy of Solids. CRC Press. 2008. ISBN 9781420008425
- G. Bunker. 2010. Introduction to XAFS - A Practical Guide to X-ray Absorption Fine Structure Spectroscopy. Cambridge University Press. 2010. ISBN 978-0-511-77001-2

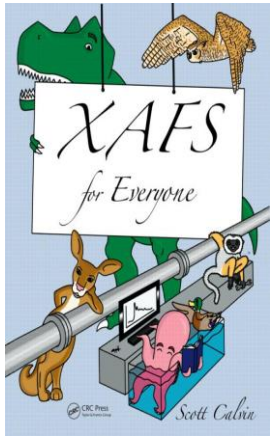

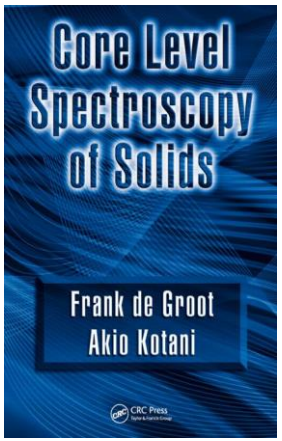

ONLINE RESOURCES (EXTRAS):

- B. Ravel, M. Newville. 2005. ATHENA, ARTEMIS, HEPHAESTUS: data analysis for X-ray absorption spectroscopy using IFEFFIT. J. Synchrotron Radiation. 2005, Volume 12, Issue 4, p. 537-541. DOI: 10.1107/S0909049505012719
- (See https://speakerdeck.com/bruceravel & https://bruceravel.github.io/demeter/ -DOCS Section-)